Integrated Radar and Communication System Design Based on Constant Envelope Waveform

Hao Lu[1], Yu Zhou[2], Yue Liu[1(✉)], Rui Li[1], and Ning Cao[1]

[1] Hohai University, Nanjing 210098, China
luhao@hhu.edu.cn
[2] State Grid Jiangsu Electric Power Co., Ltd.
Marketing Service Center, Nanjing, China

Abstract. To perform both radar and communication functions for multiuser and improve the effectiveness of power resources, a novel integrated system based on a constant envelope waveform is proposed. In this system, first, the integrated waveform combining discrete Fourier transform spread orthogonal frequency-division multiplexing (DFT-s OFDM) and continuous phase modulation (CPM), referred as DFT-s OFDM-CPM, is generated to achieve 0 dB peak to average power ratio (PAPR). Second, the detailed communication receiver and radar processing is provided. Finally, the experiment verifies the effectiveness of the proposed integrated system and its superiority to the widely used constant envelope OFDM (CE-OFDM) integrated waveform.

Keywords: Radar-communication integration · Waveform design · Continuous phase modulation · Orthogonal frequency division multiplexing · Ant lion optimizer

1 Introduction

The rapid increment of user's quantity and quality put forward a demanding requirement for the radio frequency spectrum. The concept of radar-communication integration has been seen as a promising solution to this radio frequency congestion by allowing radar and communication to share the same resources and operate in a single platform [1,2]. Among various radar and communication co-existence schemes, incorporating information bearing symbols into radar emission to form an integrated waveform is an effective approach. It can perform radar and communication functions at the same time without interference [3,4].

Currently, with more degrees of freedom in waveform synthesis and flexibility inherent to orthogonal multiple access, multicarrier waveform design represented

Q. Guo et al. (Eds.): WiSATS 2021, LNICST 410, pp. 780–789, 2022.
https://doi.org/10.1007/978-3-030-93398-2_68

by orthogonal frequency division multiplexing (OFDM) is gaining interest. Multiobjective optimal waveform design for OFDM integrated radar and communication systems is presented in [5]. The optimization of radar performance within the structure imposed by a coded OFDM format required to achieve an acceptable communication link is considered in [6]. Power minimization-based robust OFDM radar waveform design for radar and communication systems in coexistence is considered in [7]. An adaptive orthogonal frequency division multiplexing integrated radar and communications waveform design method is proposed in [8].

The above research has greatly promoted the development of joint radar-communication systems based on OFDM, but further study is still needed. Since OFDM signal is the sum of many subcarriers component via inverse discrete Fourier transform (IDFT), it has a high peak to average power ratio (PAPR) problem. This may result in the signal distortion and spectrum expansion. Besides, high power amplifier in radar transmitter may not be driven into saturation and then the power efficiency will be reduced [9]. Therefore, constant envelope OFDM (CE-OFDM) is proposed in [10] using OFDM signal to modulate phase. Nevertheless, this can not maintain the usage of subcarriers' orthogonality which means that some advantages of OFDM such as low complexity frequency equalization, frequency multiplexing and so on cannot be used.

In this letter, to address the high PAPR problem, a novel radar-communication integrated system is proposed. Advantages of this system include three points. First, discrete Fourier transform spread orthogonal frequency-division multiplexing (DFT-s OFDM) and continuous phase modulation (CPM) are combined to generate an integrated waveform, DFT-s OFDM-CPM, with constant envelope. This operation allows the power amplifier in radar transmitter working in a saturated region, gaining farther effective working distance and better performance. Second, the spread spectrum and interleaved frequency division multiple access (I-FDMA) subcarrier mapping methods enable the proposed system to allow multiple users to work simultaneously and due to the orthogonality between the subcarriers, there will be no interference between users. Third, to eliminate the dependence of radar detection performance on the transmitted symbol, radar processor in frequency domain is carried out. Simulation results show that the proposed system can realize the superior performance both in radar and communication.

This paper is organized as follows. System framework and workflow are introduced in Sect. 2. Simulation results are given in Sect. 3 and Sect. 4 concludes this letter.

2 System Model

2.1 Basic Framework of Integrated System

Considering a traffic controlling scenario (Fig. 1), there is a control center containing U controllers and each controller manages one or more ship targets.

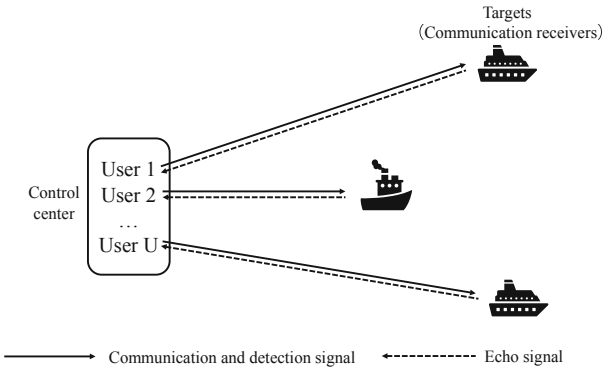

Fig. 1. Typical operational scenario.

U managers need to send commands to the targets and keep track of the targets' states including their position and speed. Each target, i.e., communication receiver is asked to decode commands and preform related operations after receiving the signal.

Firstly, the controller u sends integrated signal $x_u(t)$ to realize information transmission and targets tracking,

$$x_u(t) = \exp(j2\pi f_c t) \sum_{\mu=0}^{N_s-1} \sum_{n=0}^{K-1} S_{Tu}(\mu, n) \exp(j2\pi f_n t) \cdot \mathrm{rect}(\frac{t - \mu T_s}{T_s}) \tag{1}$$

where f_c is the carrier frequency; N_s is the number of OFDM symbols contained in each pulse; K is the subcarriers number contained in one time block; T_s is the OFDM symbol duration; $f_n = n\Delta f$, $\Delta f = \frac{1}{T_s}$ is the frequency interval between subcarrier. $S_{Tu}(\mu, n)$ denotes the code in the n^{th} subcarrier of the μ^{th} symbol. We consider that a constant envelope waveform may be achieved through replacing these conventional data symbols with samples from a CPM waveform in time domain. The specific operations is given in the next subsection.

2.2 Generation of Data Symbols

Fig. 2. Signal model.

For convenience, we discuss the generation of data symbols of user u in one time block. The signal model is shown in Fig. 2. Firstly, we give the CPM signal definition [11],

$$s(t,\beta) = \exp(j\phi(t;\beta)). \tag{2}$$

$\phi(t;\beta)$ is the signal phase,

$$\phi(t;\beta) = 2\pi h \sum_i \beta_i q(t - iT), \tag{3}$$

where h is the modulation index, information symbols $\beta_i \in \{\pm 1, \cdots, \pm(M-1)\}$ and M is modulation order. $q(t)$ is the phase shaping function. The derivative of $q(t)$ is called the frequency shaping function and is denoted by $g(t)$. The function $g(t)$ has a support of L symbol intervals and an underlying area of 1/2. This paper considers the full response CPM with $L = 1$.

We observe $s(t;\beta)$ over JT seconds (J is an integer) and sample at rate $f_{sa} = N/T$ to generate the vector of signal samples $\boldsymbol{s} = [s_0 \cdots s_{JN-1}]^{\mathrm{T}} = [s(t = \frac{0N}{T};\beta) \cdots s(t = \frac{(JN-1)N}{T};\beta)]^{\mathrm{T}}$. Then, we pass the sampled output into JN-point DFT,

$$S_i = \sum_{n=0}^{JN-1} s_n \exp(\frac{-j2\pi in}{NJ}), \tag{4}$$

where $i = 1, \cdots, JN-1$ denotes the discrete frequency index. The DFT outputs will be treated as the data symbols in each subcarrier of OFDM. The key observation is this, if the time domain symbols at DFT input are constant modulus, then the time-domain symbols at the IDFT output will also be constant modulus.

Each user obtains the data symbols according to the above steps and maps them into subcarriers of IDFT using I-FDMA approach [12], where the subcarriers are equally spaced over the entire system bandwidth,

$$S_{Tu}(1,n) = \begin{cases} S_i, \, n = u + iU \\ 0, \quad \text{otherwise} \end{cases} \tag{5}$$

where $n = 1, \cdots, K$, $K = UJN$. I-FDMA mapping maintains the input time symbols in each sample and has lower PAPR [13]. Besides, due to the orthogonality between subcarriers, the interference between different users can be avoided. Therefor, the transmitted waveform (1) is expected to own constant envelope in each time block and be friendly toward the use of nonlinear radar transmitter. We refer this waveform as DFT-s OFDM-CPM.

2.3 Communication Receiver

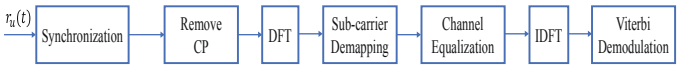

Fig. 3. Communication receiver.

Each target is seen as a communication receiver to receive and decode the controller's commands. As shown in Fig. 3, they receive the integrated signal

$$r_u(t) = h(t) * x_u(t) \exp(j2\pi\epsilon t) + w(t), \tag{6}$$

where ρ and ϵ represent time and frequency offset, respectively. $h(t)$ represents the channel impulse response and $w(t)$ is awgn. The receiving end first performs symbol positioning and frequency compensation through the CP-based ML maximum likelihood synchronization algorithm. Then remove the CP and perform DFT and inverse mapping to obtain the symbol of user u in the frequency domain. If the frequency selection channel is used, the receiver needs to equalize the received signal. Here, the receiver can use MMSE frequency domain equalization with lower complexity. The equalized signal is transformed into the time domain by IDFT, and finally the famous VA algorithm [11] is used to obtain the transmitted CPM symbol.

2.4 Radar Processing in Frequency Domain

Assuming a moving target managed by user u is at the range R with relative velocity v, the user u receives the target echo is,

$$\begin{aligned} y_u(t) &= \sum_{\mu=0}^{N_s-1} \sum_{n=0}^{K-1} S_{Ru}(\mu, n) \exp(j2\pi f_n t) \mathrm{rect}(\frac{t-\mu T_s}{T_s}) \\ &= \sum_{\mu=0}^{N_s-1} \sum_{n=0}^{K-1} S_{Tu}(\mu, n) \exp(j2\pi\mu f_d T_s) \\ &\quad \cdot \exp(-j2\pi f_n \frac{2R}{c}) \exp(j2\pi f_n t) \mathrm{rect}(\frac{t-\mu T-\frac{2R}{c}}{T_s}), \end{aligned} \tag{7}$$

where c is the speed of light and f_d denotes the Doppler frequency shift caused by the targets movement.

Since the information code on some subcarriers in each user's transmitted waveform is 0, the traditional radar detection method that relies on symbol correlation is no longer applicable. To eliminate the dependence of radar processing on the correlation of the transmitted information, we can compare the transmitted information $S_{Tu}(\mu, n)$ and the received information $S_{Ru}(\mu, n)$ at the output of the $y(t)$ de-multiplexer to obtain targets' states. The frequency domain channel transfer function is given by calculating an element-wise division,

$$\begin{aligned} D(\mu, n) &= \frac{S_{Ru}(\mu, n)}{S_{Tu}(\mu, n)} \\ &= \exp(j2\pi\mu f_d T_s) \exp(-j2\pi f_n \frac{2R}{c}). \end{aligned} \tag{8}$$

It is evident that the range and Doppler influences are orthogonal. We denote $k_R(n) = \exp(j2\pi f_n \frac{2R}{c})$ and $k_D(\mu) = \exp(j2\pi\mu f_d T_s)$. Note that we only operate on DFT-s OFDM-CPM subcarriers that contain data information. Assuming $U = 2$, range of target can be calculated through IDFT of $k_R(n)$,

$$r(p) = \text{IDFT}(k_R(n)) = \frac{1}{JN} \sum_{n=0}^{JN-1} k_R(2n) \exp(j2\pi \frac{n}{JN} p), \tag{9}$$

with $p = 0, \cdots, JN-1$. A peak of $r(p)$ will occur at $p = \lfloor \frac{2R\Delta f K}{c} \rfloor$. The relative velocity can be solved in a similar method to $k_v(\mu)$ and a peak will occur in the $\lfloor \frac{2v f_c N_s}{\delta f c} \rfloor$.

3 Simulation Results

In this section, the performance of the integrated system in communication and detection is illustrated with the spectral efficiency (SE), bit error rate (BER) as well as radar range and velocity profile. Without loss of generality, we consider an integrated system operating with the parameter setting: carrier frequency $f_c = 24\,\text{GHz}$; frequency interval $\Delta f = 400\,\text{kHz}$; user number $U = 2$; symbols of each user $J = 40$; symbol number $N_s = 5$; sample number $N_{sa} = 2$; CP length $N_{cp} = 20$; frequency offset $\epsilon = 0.25$; the modulation order M = 4; modulation index $h = 1/4$. We consider AWGN channel. For reference, performance of conventional OFDM modulated by 8PSK and the well known constant envelope OFDM (CE-OFDM) [10] by phase modulating OFDM are also assessed.

Firstly, We give the signal normalized amplitude comparison in Fig. 4. We can see that the DFT-s OFDM-CPM maintains the constant envelope as that of CE-OFDM while OFDM has a large amplitude variation.

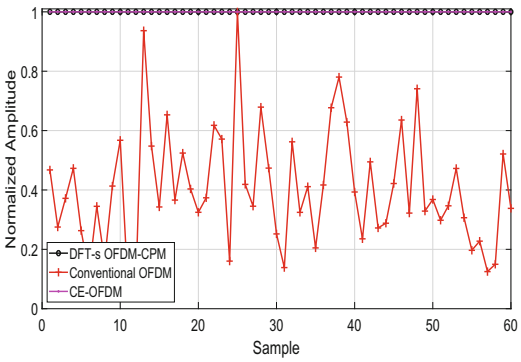

Fig. 4. Signal normalized amplitude comparison.

3.1 Spectral Efficiency

SE is defined as $SE = \frac{R_b}{W}$, where R_b is the bit rate and W is the signal occupied bandwidth. For one thing, we consider the bit rate of the three modulations. The bit rate of OFDM is $R_b = N_c \log_2 M/T(b/s)$. Since DFT-s OFDM-CPM needs to sample symbol of the original CPM signal with two points, the signal rate is $R_b/2$. In addition, in order to ensure that the input of the phase modulator is a real number, the input to the IDFT is a conjugate symmetric, zero-padded data vector, so its bit rate is less than $R_b/2$. For another, the bandwidth occupied by DFT-s OFDM-CPM and traditional OFDM is $W = N_c * \Delta f$. Because CE-OFDM requires phase modulation of the OFDM signal. Its bandwidth is $B = \max(2\pi h, W)$Hz. Therefore, when $h = 1/4$, the highest spectral efficiency is OFDM, DFT-s OFDM -CPM is higher than CE-OFDM. According to the parameter settings, the spectral efficiency of the three modulation methods is shown in Table 1.

Table 1. Spectral efficiency of the three modulations

Modulations	SE (bits/s/Hz)
DFT-s OFDM-CPM	1
Conventional OFDM	2
CE-OFDM	0.637

3.2 BER Performance Comparison

Here, BER performance comparison between the three modulation methods is provided in Fig. 5. First, under the premise of perfect frequency synchronization, we can see that the DFT-s OFDM-CPM has the best BER performance. The demodulation process depends on the demodulation of symbol in each subcarrier after a series of operations opposite to the transmitter. Thus, due to the symbol memory inherent in CPM, the BER performance of DFT-s OFDM-CPM is outstanding. Then, considering frequency shift synchronization. To maintain the constant envelope of DFT-s OFDM-CPM, CP-based ML synchronization [14] without additional training sequences is introduced here. The Gaussian weighted average of the estimated frequency shift value of each symbol is used as the final frequency shift estimation. Among the three methods, CE-OFDM is least sensitive to imperfect frequency synchronization due to its phase modulation and unwrapping operations. Both DFT-s OFDM-CPM and traditional OFDM are sensitive to carrier frequency offset (CFO).

3.3 Radar Detection Performance

Considering one controller manages two targets with distance 28 m, velocity 650 m/s and distance 33 m, velocity 350 m/s, respectively. The radar range profile

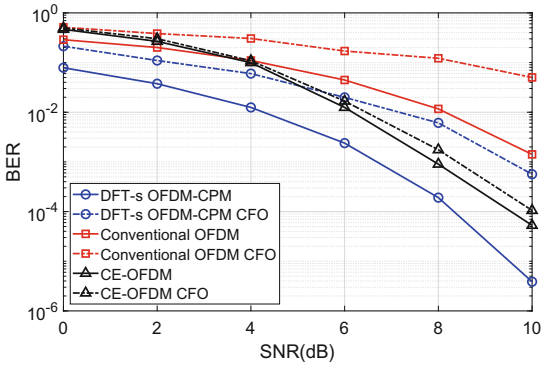

Fig. 5. BER comparison under AWGN channel.

comparison is given in Fig. 6. Assuming the same amount of transmitted data symbols, we can see that only the two main peaks in 28m and 33m of the DFT-s OFDM-CPM are prominent, the middle depression is about 20dB, and the side lobe is the lowest. It can well distinguish targets 5m apart. The range resolution of the radar is inversely related to the number of subcarriers. Considering the number of transmitted data symbols is J, the number of subcarriers of DFT-s OFDM-CPM is UJN, CE-OFDM is $2J + 2$, and OFDM is J. Therefore, the radar range resolution of DFT-s OFDM-CPM is optimal.

Finally, the velocity profile comparison is given in Fig. 7. The proposed system exhibits the similar velocity resolution performance to that of conventional OFDM with about 13 dB drop between two targets. This paper focuses on distance resolution. Different application scenarios can adjust parameters according to their own needs to obtain the required resolution.

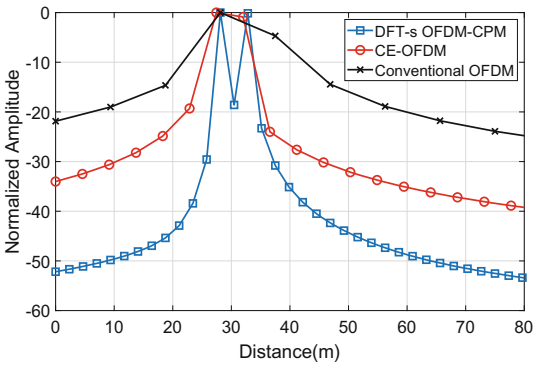

Fig. 6. Radar range profile.

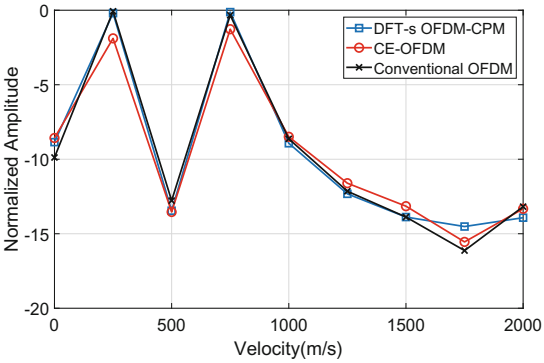

Fig. 7. Radar velocity profile.

4 Conclusion

In this letter, a DFT-s OFDM-CPM scheme for an joint radar-communication system is studied to solve the high PAPR problem. The detailed communication and radar processing are provided. The proposed system exhibits competitive communication and radar performance. We believe that our design may contribute to improving radar and communication integration performance. Future work will entail refining our model by considering different kinds of channel and enhancing the robustness to the frequency shift.

Acknowledgements. This work was supported by Research on Performance Evaluation and Optimization Technology of Local IOT for Client-side Metering Equipment under grant No. 5700-202118203A-0-0-00.

References

1. Chiriyath, A.R., Paul, B., Bliss, D.W.: Radar-communications convergence: coexistence, cooperation, and co-design. IEEE Trans. Cogn. Commun. Netw. **3**(1), 1–12 (2017)
2. Sturm, C., Wiesbeck, W.: Waveform design and signal processing aspects for fusion of wireless communications and radar sensing. Proc. IEEE **99**(7), 1236–1259 (2011)
3. Li, Q., Dai, K., Zhang, Y., Zhang, H.: Integrated waveform for a joint radar-communication system with high-speed transmission. IEEE Wirel. Commun. Lett. **8**(4), 1208–1211 (2019)
4. Zhang, Q., Zhou, Y., Zhang, L., Gu, Y., Zhang, J.: Waveform design for a dual-function radar-communication system based on CE-OFDM-PM signal. IET Radar Sonar Navig. **13**(4), 566–572 (2018)
5. Liu, Y., Liao, G., Yang, Z., Xu, J.: Multiobjective optimal waveform design for OFDM integrated radar and communication systems. Signal Process. **141**, 331–342 (2017)
6. Ellinger, J., Zhang, Z., Wu, Z., Wicks, M.C.: Dual-use multicarrier waveform for radar detection and communication. IEEE Trans. Aerosp. Electron. Syst. **54**(3), 1265–1278 (2017)

7. Shi, C., Wang, F., Sellathurai, M., Zhou, J., Salous, S.: Power minimization-based robust OFDM radar waveform design for radar and communication systems in coexistence. IEEE Trans. Signal Process. **66**(5), 1316–1330 (2017)
8. Liu, Y., Liao, G., Xu, J., Yang, Z., Zhang, Y.: Adaptive OFDM integrated radar and communications waveform design based on information theory. IEEE Commun. Lett. **21**(10), 2174–2177 (2017)
9. Wylie-Green, M.P., Perrins, E., Svensson, T.: Introduction to CPM-SC-FDMA: a novel multiple-access power-efficient transmission scheme. IEEE Trans. Commun. **59**(7), 1904–1915 (2011)
10. Huang, Y., et al.: Constant envelope OFDM RadCom fusion system. EURASIP J. Wirel. Commun. Netw. **2018**(1), 104 (2018)
11. Anderson, J.B., Aulin, T., Sundberg, C.E.: Digital Phase Modulation. Springer, Heidelberg (2013)
12. Sorger, U., De Broeck, I., Schnell, M.: Interleaved FDMA-a new spread-spectrum multiple-access scheme. In: 1998 IEEE International Conference on Communications, Conference Record, Affiliated with SUPERCOMM 1998, ICC 1998 (Cat. No. 98CH36220), vol. 2, pp. 1013–1017, June 1998
13. Myung, H.G., Goodman, D.J.: Single Carrier FDMA: A New Air Interface for Long Term Evolution, vol. 8. Wiley, Hoboken (2008)
14. Doğan, H., Odabaşıoğlu, N., Karakaya, B.: Time and frequency synchronization with channel estimation for SC-FDMA systems over time-varying channels. Wirel. Pers. Commun. **96**(1), 163–181 (2017)